

Electronic Supplementary Information:

Insight into the electrocatalytic activation of peroxymonosulfate by a Ti/MnO₂ anode via one-step electrodeposition approach toward the degradation of levofloxacin

Wenzhi Zhang^a, Zhang Hao^a, Guohua Dong^{a,*}, Zhuanfang Zhang^a, Dong-Feng Chai^{a,*},
Ming Zhao^{a,b}, Jinlong Li^{a,c}, Han Wu^a and Xu Hou^a

Contents

Text S1 Characterization of electrodes

Text S2 Electrocatalytic degradation of LFX

Fig. S1 The effects of different preparation conditions on the degradation of LFX.

Fig. S2 UV-vis spectra of LFX at pre-scheduled time intervals after electrocatalytic degradation by MnO₂-EC/PMS system under optimal conditions.

Fig. S3 Mass spectra graphs of intermediates of the LFX degradation.

Table S1 The identified possible intermediates during LFX degradation from the LC-MS data.

Text S1. Characterization of electrodes

The morphology and elemental composition of the Ti/MnO₂ electrocatalyst film were investigated by scanning electron microscopy (SEM, Hitachi, S-4300, Japan) coupled with energy-dispersive X-ray spectroscopy (EDS, X-Max 20 Aztec energy, Britain). X-ray diffraction (XRD) patterns were recorded on an X-ray diffractometer (XRD, Bruker, AXS (D8), Germany) using Cu K α ($\lambda=1.54$ Å) as the x-ray source with a 2θ range of 10° to 90°, operating at 60 kV and 80 mA. X-ray photoelectron spectroscopy (XPS) was collected on an electron spectrometer (XPS, VG, EscaLab 250 Xi, UK) with Al K α radiation (300 W, $h\nu = 1486.6$ eV) as an X-ray source. The obtained data were calibrated with standard C 1 s (C-C bond) with a binding energy of 284.8 eV. Fourier transform infrared spectra (FTIR) were gained by the Fourier transform infrared spectrophotometer (FTIR, PE, US) in the range of 4000-400 cm⁻¹. The absorbance of LFX solution was recorded with an ultraviolet-visible dual-beam spectrophotometer (UV-vis, Persee, TU-1900, China) at the maximum absorption wavelength of LFX. The reacted intermediates were analyzed by liquid chromatography / mass spectrometry (LC-MS, Agilent, LC1200/MS6310, USA). The standard three-electrode electrochemical system was employed to investigate the electrochemical properties of the obtained Ti/MnO₂ electrocatalyst anode on an electrochemical workstation (CHI660E, Chenhua, Shanghai), in which the Ti/MnO₂ electrode, platinum foil and Ag/AgCl electrode were used as the working electrode, counter electrode and reference electrode, respectively. Cyclic voltammetry (CV) tests were performed for checking the degradation process in 0.1 mol·L⁻¹ sodium sulfate, a mixed solution of 10 mg·L⁻¹ LFX and 0.1 mol·L⁻¹ sodium sulfate, and a mixed solution of 10 mg·L⁻¹ LFX and 0.1 mol·L⁻¹ sodium sulfate and 1.0 g·L⁻¹ PMS as an electrolyte solution, respectively, in a voltage range of -1.0~2.0 V (vs. Ag/AgCl) at a scan rate of 50 mV·s⁻¹. The catalyst loading on the Ti substrate surface was determined by dividing the total mass of catalyst deposited on the electrode by the effective electrode area, with units expressed as g·cm⁻². It is worth noting that the total mass of catalyst on the electrode was obtained through pre- and post-deposition weighing of the electrodes.

Text S2. Electrocatalytic degradation of LFX

The LFX degradation experiments were carried out in a 50 mL beaker as reaction cell with or without existence of PMS and Ti/MnO₂ anode. For initially comparing and evaluating the role of MnO₂ catalyst, PMS and electrocatalysis (EC), five different systems were designed and adopted to degrade the LFX: i) PMS alone (only existence of PMS in LFX solution), ii) the conventional MnO₂ electrocatalysis system (MnO₂-EC, Ti/MnO₂ and stainless-steel as anode and cathode in LFX solution respectively), iii) MnO₂/PMS system (MnO₂ granules dispersed into the PMS+LFX solution), iv) EC/PMS system (Ti sheets as the anode and stainless-steel as the cathode in LFX solution) and v) MnO₂-EC/PMS system (Ti/MnO₂ and stainless-steel as anode and cathode in PMS+LFX solution respectively). The above whole degradation operating conditions are 0.1 mol·L⁻¹ sodium sulfate solution, Na₂SO₄ (pH=7) 30 mA·cm⁻² of applied current density, the electrode plate distance 1 cm, pH value of 7, 0.3g·L⁻¹ PMS and 30 mg·L⁻¹ LFX. In contrast, the degradation only with the PMS activation was performed without any electrocatalyst electrode.

The concentrations of the LFX solutions before and after degradation were gained by measuring the UV-vis spectra of LFX wastewater at the characteristic adsorption peak with fixed time intervals employing the Ultraviolet-visible spectrophotometer. For achieving the optimal degradation effect, the initial antibiotic concentration of LFX (10-40 mg·L⁻¹), PMS concentration (0.06-1.2g·L⁻¹), current density (20-50 mA·cm⁻²), electrode plate distance (0.5-3 cm), pH value (3-11), and other basic operation parameters were systematically optimized. It should be noted that the initial pH value of the simulated aqueous solution was adjusted by 0.1 M H₂SO₄ or 0.1 M NaOH.^{6, 7} The reactive oxygen species (ROS) generated in LFX degradation process were evaluated by using methanol (MeOH) as the scavenger of ·OH and SO₄·⁻, and tert-butyl alcohol (TBA) as the scavenger of ·OH.⁴

The degradation efficiency (η) was calculated based on the following equation (Eq.

1):

$$\eta = \frac{C_0 - C_t}{C_0} \times 100\% = \frac{A_0 - A_t}{A_0} \times 100\% \quad (1)$$

Where C_0 and C_t are the concentration of LEX (mg L⁻¹) at reaction time of 0 and t,

A_0 and A_t are the absorbance of LFX at reaction time 0 and t, respectively.^{5,10}

The kinetic of electrocatalytic degradation of LFX is described by the first-order kinetic equation (Eq. 2):

$$\ln \frac{C_0}{C_t} = kt \quad (2)$$

Where C_0 and C_t resemble the physical quantity in Eq. 1. k denotes the apparent rate constants (min^{-1}).²

The mineralization of the LFX was evaluated by measuring the removal rate of Chemical oxygen demand (COD) based on a standard method (Eq. 3).^{8,9}

$$\eta(\text{COD},\%) = \frac{\text{COD}_0 - \text{COD}_t}{\text{COD}_0} \times 100\% \quad (3)$$

Where COD_0 is the COD values at the initial 0 minute and t minute after reaction, respectively.

By measuring the COD values at different time intervals, the average current efficiency (ACE) was calculated by the following formula (Eq. 4).

$$\text{ACE} = \frac{[(\text{COD})_t - (\text{COD})_{t+\Delta t}]}{8I\Delta t} \times 100\% \quad (4)$$

The instantaneous current efficiency (ICE) was calculated from Faraday 's law by measuring the COD values at different time intervals (Eq. 5).

$$\text{ICE} = \frac{(\Delta\text{COD})_t FV}{8I\Delta t} \times 100\% \quad (5)$$

By measuring the COD values at different time intervals, the electrochemical energy consumption (EEC) was estimated by the following formula (Eq. 6).

$$\text{EEC} = \frac{Uit}{V(\Delta\text{COD})_t} \quad (6)$$

Where COD_t and $\text{COD}_{t+\Delta t}$ are the COD values at time t and t+ Δt (mg L^{-1}), respectively. F is Faraday constant ($964875 \text{ C mol}^{-1}$), V is the volume of electrolyte (L), constant 8 is the oxygen equivalent mass, I is the current (A), Δt is the electrolysis time (h), and U is the average cell potential (V).¹

The results and discussion in Fig. S1

In Fig. S1a, the degradation efficiencies of LFX in 120 min were 57.03 %, 63.02

%, 65.56 % and 62.29 %, respectively, indicating that $120\text{g}\cdot\text{L}^{-1}$ was the optimal concentration of the precursor solution. In Fig. S1b, the degradation efficiencies of LFX in 120 min were 63.35 %, 68.15 %, and 65.37 %, respectively. When the electrodeposition time of the catalyst is 35 min, the degradation efficiency is the highest. The deposition time of 35 min increases the number of sites for activating PMS, but too long electrodeposition time will lead to an increase in catalyst loading, which will affect the charge transfer and reduce the degradation efficiency.^{2, 3} After calculation, the MnO_2 loading amounts on the Ti substrate is $\sim 0.1293\text{ g}\cdot\text{cm}^{-2}$ for the optimal MnO_2 electrode.

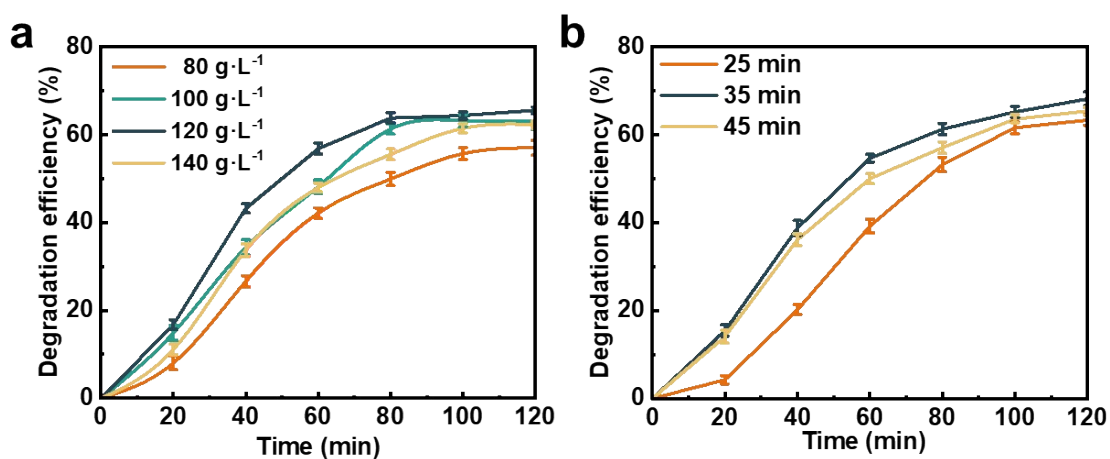


Fig. S1 The effects of different preparation conditions on the degradation of LFX: (a) MnSO_4 concentration, (b) electrodeposition time.

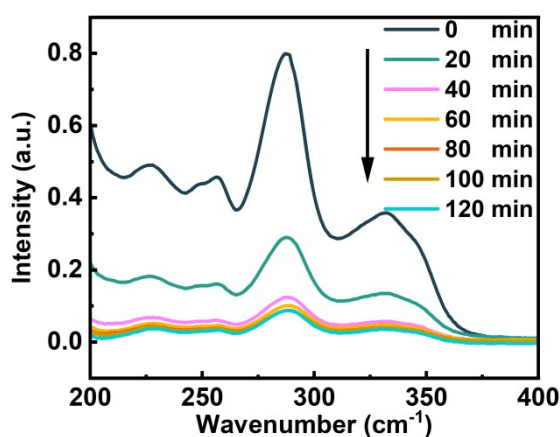
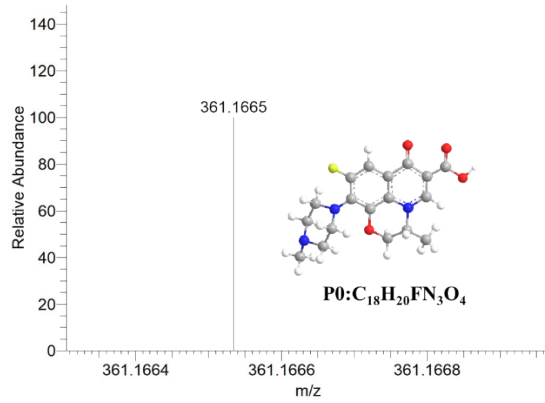
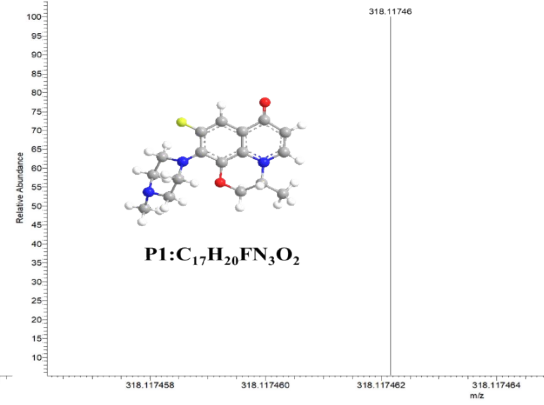


Fig. S2 UV-vis spectra of LFX at pre-scheduled time intervals after electrocatalytic degradation by $\text{MnO}_2\text{-EC/PMS}$ system under optimal conditions.

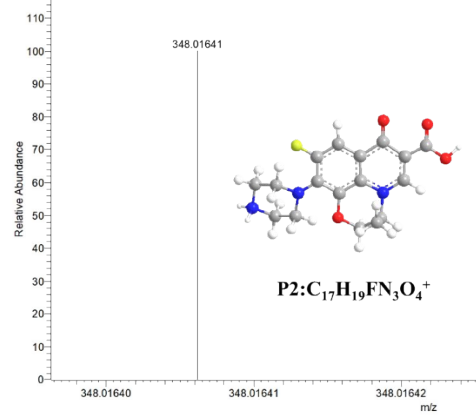
20221012_DLL_2_#981 RT: 10.05 AV: 1 NL: 1.69E4
T: FTMS - c ESI Full ms [50.0000-600.0000]



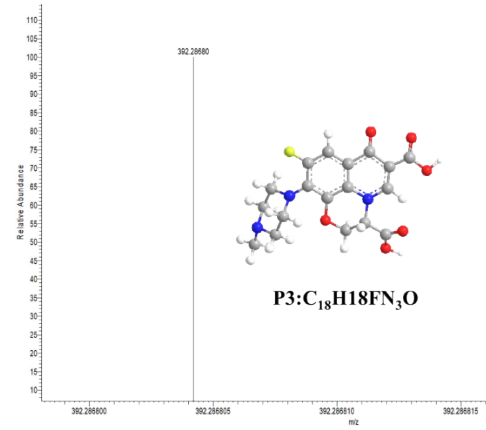
20221014_ZH_1#2 RT: 0.02 AV: 1 NL: 2.51E4
T: FTMS - c ESI Full ms [50.0000-600.0000]



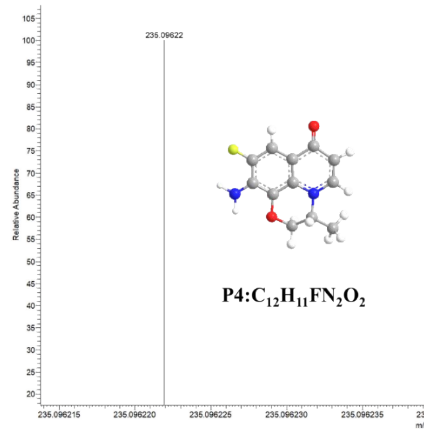
20221014_ZH_1#1484-1496 RT: 14.89-15.01 AV: 13 NL: 1.27E3
T: FTMS - c ESI Full ms [50.0000-600.0000]



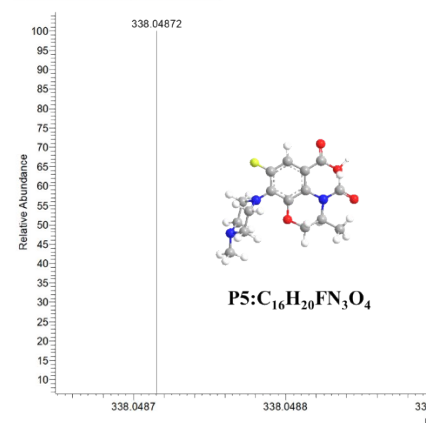
20221014_ZH_1#2 RT: 0.02 AV: 1 NL: 4.90E4
T: FTMS - c ESI Full ms [50.0000-600.0000]



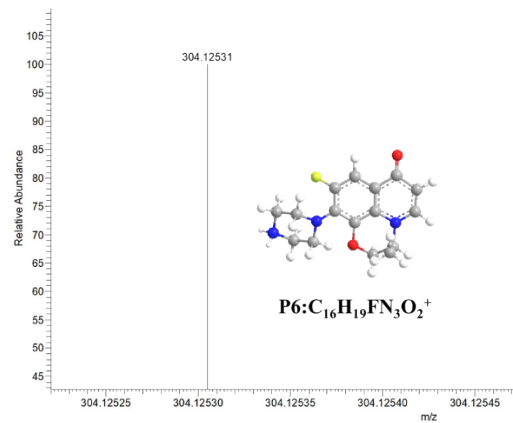
20221014_ZH_1#2 RT: 0.02 AV: 1 NL: 3.90E4
T: FTMS - c ESI Full ms [50.0000-600.0000]



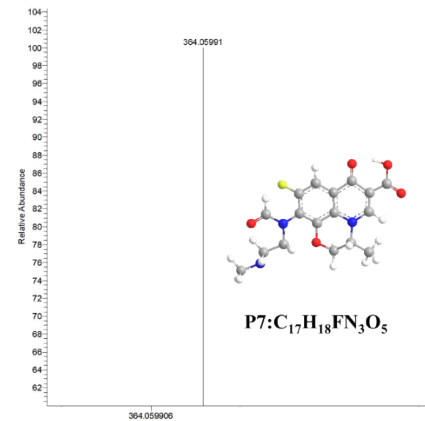
20221014_ZH_1#1484-1496 RT: 14.89-15.01 AV: 13 NL: 3.50E4
T: FTMS - c ESI Full ms [50.0000-600.0000]



20221014_ZH_1#1484-1496 RT: 14.89-15.01 AV: 13 NL: 1.12E3
T: FTMS - c ESI Full ms [50.0000-600.0000]



20221014_ZH_1#2 RT: 0.02 AV: 1 NL: 2.62E4
T: FTMS - c ESI Full ms [50.0000-600.0000]



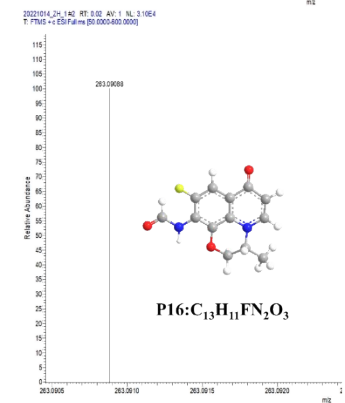
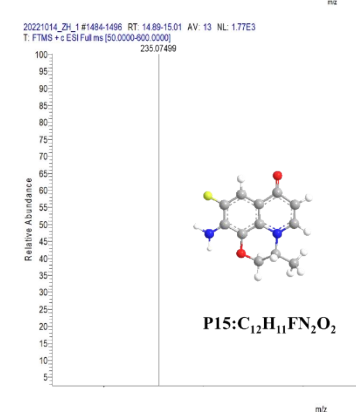
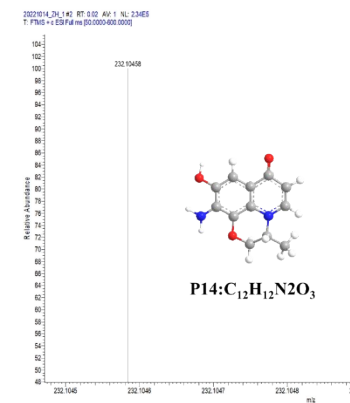
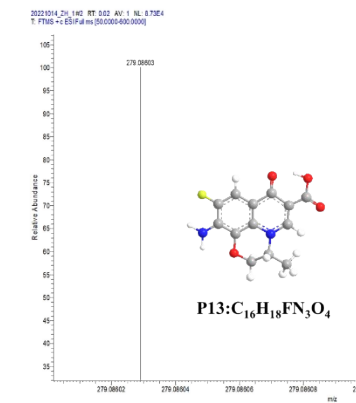
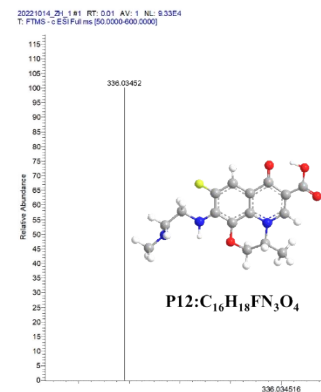
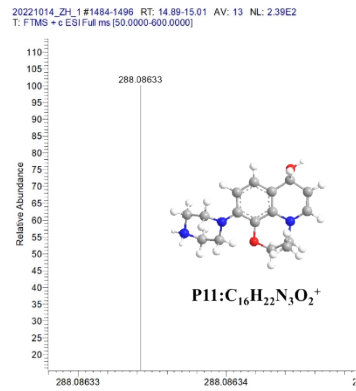
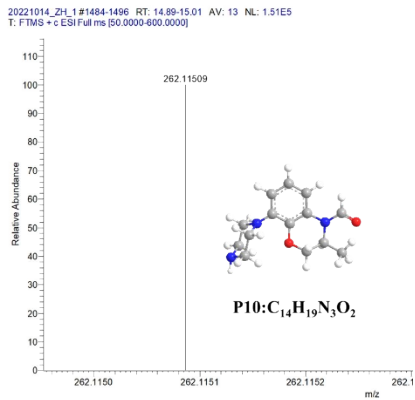
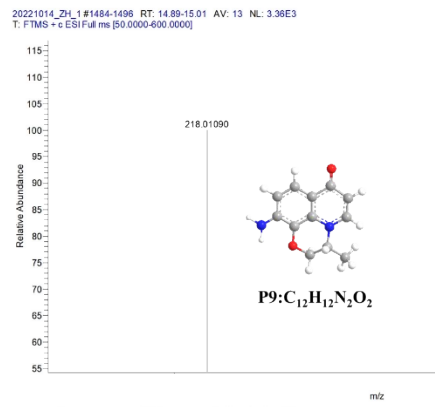
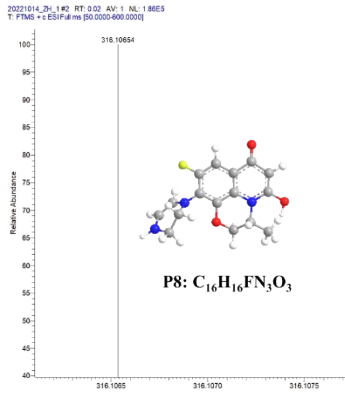
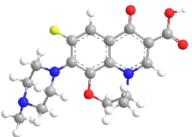
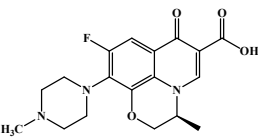
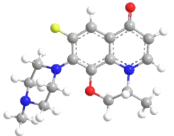
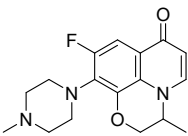

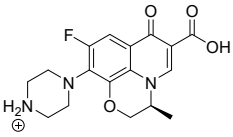
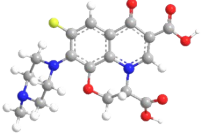
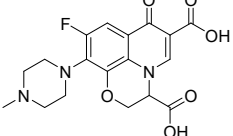

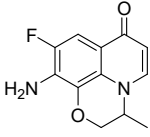
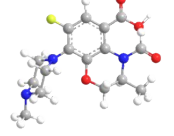
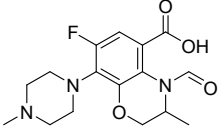
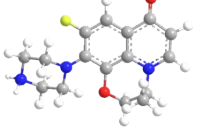
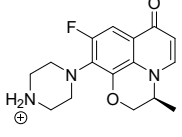
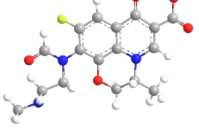
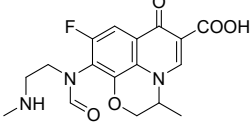
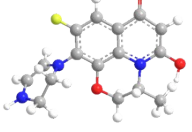
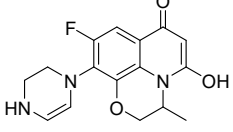
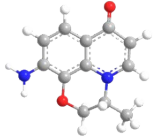
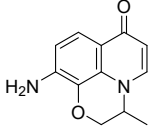
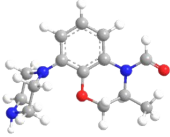
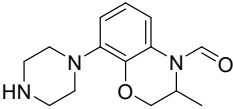
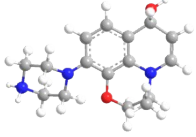
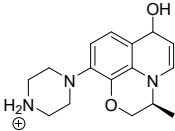

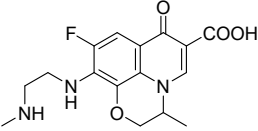
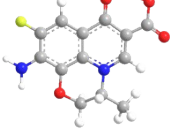
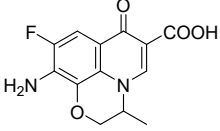
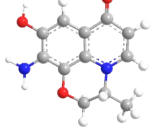
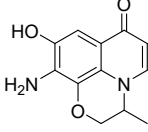
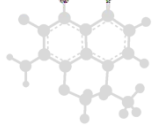
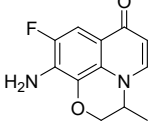
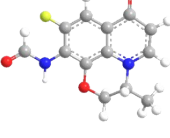
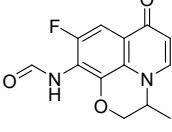


Fig. S3 Mass spectra graphs of intermediates of the LFX degradation.

Table S1. The identified possible intermediates during LFX degradation from the LC-MS data.

Name	Empirical formula	3D Molecular structure	Molecular structure	Exact m/z value
P0	$C_{18}H_{20}FN_3O_4$			361
P1	$C_{17}H_{20}FN_3O_2$			318
P2	$C_{17}H_{19}FN_3O_4^+$			348
P3	$C_{18}H_{18}FN_3O_6$			392
P4	$C_{12}H_{11}FN_2O_2$			235
P5	$C_{16}H_{20}FN_3O_4$			338
P6	$C_{16}H_{19}FN_3O_2^+$			304
P7	$C_{17}H_{18}FN_3O_5$			364
P8	$C_{16}H_{16}FN_3O_3$			316

P9	$C_{12}H_{12}N_2O_2$			218
P10	$C_{14}H_{19}N_3O_2$			262
P11	$C_{16}H_{22}N_3O_2^+$			288
P12	$C_{16}H_{18}FN_3O_4$			336
P13	$C_{16}H_{18}FN_3O_4$			279
P14	$C_{12}H_{12}N_2O_3$			232
P15	$C_{12}H_{11}FN_2O_2$			235
P16	$C_{13}H_{11}FN_2O_3$			263

References

- 1 A. Rahmani, A. Ansari, A. Seid-mohammadi, M. Leili, D. Nematollahi and A. Shabanloo, *Journal of Environmental Chemical Engineering*, 2023, **11**, 109118.
- 2 Y. Ni, W. Yue, F. Liu, W. Bi, Z. Sun and Y. Wu, *Colloids and Surfaces A: Physicochemical and Engineering Aspects*, 2023, **666**, 131318.
- 3 L. Jin, Y. Huang, H. Liu, L. Ye, X. Liu and D. Huang, *Journal of Hazardous*

- Materials*, 2024, **463**, 132904.
- 4 J. Zhang, Y. Li, C. Liu, C. Zhu, C. shao and Y. Zhao, *Journal of Molecular Structure*, 2023, **1276**, 134822.
 - 5 L. Liu, Y. Li, C. Zhu, J. Zhang and L. Chen, *Optical Materials*, 2023, **143**, 114200.
 - 6 L. Dong, Z. Zhuang, G. Dong, H. Zhang, M. Zhu, Z. Zhang, M. Zhao, J. Li and W. Zhang, *Journal of Environmental Chemical Engineering*, 2023, DOI: 10.1016/j.jece.2023.110865.
 - 7 M. Zargarian, A. Ansari, H. Masoumi, D. Nematollahi, A. Shabanloo, M. Eslamipanah and B. Jaleh, *Journal of Environmental Chemical Engineering*, 2023, **11**, 110280.
 - 8 T. Xu, X. Tang, M. Qiu, X. Lv, Y. Shi, Y. Zhou, Y. Xie, M. Naushad, S. S. Lam, H. S. Ng, C. Sonne and S. Ge, *Journal of Environmental Management*, 2023, **344**, 118718.
 - 9 G. Dong, K. Lang, Y. Gao, W. Zhang, D. Guo, J. Li, D.-F. Chai, L. Jing, Z. Zhang and Y. Wang, *Journal of Colloid and Interface Science*, 2022, DOI: 10.1016/j.jcis.2021.11.023.
 - 10 G. Hua, X. Zhicheng, Q. Dan, W. Dan, X. Hao, Y. Wei and J. Xiaoliang, *Chemosphere*, 2020, **261**, 128157.